STATISTICAL MODELING OF "GET" SYSTEM INSTALLED AT THE BASE OF OIL RESERVOIR

G.M. Dolgich, G.V. Anikin*, I.P. Rilo, K.A. Spasennikova*

OOO NPO "Fundamentstroyarkos", 12 Novatorov str., Tyumen, 625014, Russia; fsa@npo-fsa.ru
**Earth's Cryosphere Institute, SB RAS, 86 Malygina str., Tyumen, 625000, Russia; anikin@ikz.ru*

The state of soils under the tank with oil has been calculated. The tank oil located at the Vankor oil field is cooled by "GET" systems (horizontal system of soil temperature stabilization) produced by NPO "Fundamentstroyarkos", OOO. Considered are 48 scenarios for a two year period, each is generated by the Monte-Carlo method based on the distributions of meteorological parameters obtained by averaging of the archive data of the Igarka weather station. It has been demonstrated that variations in the ground temperature are significant for a variety of options. Thus the conventional univariant forecast becomes doubtful. In this regard a method of stochastic forecasting, which allows for the worst-case scenario and is suggested to be employed for the purpose of forecasting future processes in the frozen soil. This scenario must be considered in the design. In addition, the operation of "GET" systems is simulated, and their properties and parameters are investigated.

Soil, Monte-Carlo method, stochastic forecasting, permafrost

INTRODUCTION

When predictions for variations in permafrost soil conditions under buildings and structures are made, it has become a streamlined path to focus and rely on the same parameters repeated from year to year, such as the mean monthly air temperature, velocity of air (wind speed) and the snow cover depth. Given that the predictions tend to be long-term, doesn't it mean that only one option is ever considered? To what extent is this "intelligence about the future" justified?

To answer this question the authors have performed calculations for temperature field under the oil tank where soil is cooled with the use of soil temperature stabilization system of "GET" type [*Dolgich et al., 2008*] at the Vankor oil field, providing 48 scenarios of future processes in permafrost soil.The following parameters were determined in each of the considered scenarios: the temperature field in the computational domain covering surface sized 100 × 100 m at a depth of 10 m; duration of the period with negative air temperature; operation time of the thermostabilization system; average capacity of one condensing unit during the winter period; average running power of one condensing unit. A schematic block diagram of the computational domain and oil tank area is shown in Fig. 1.

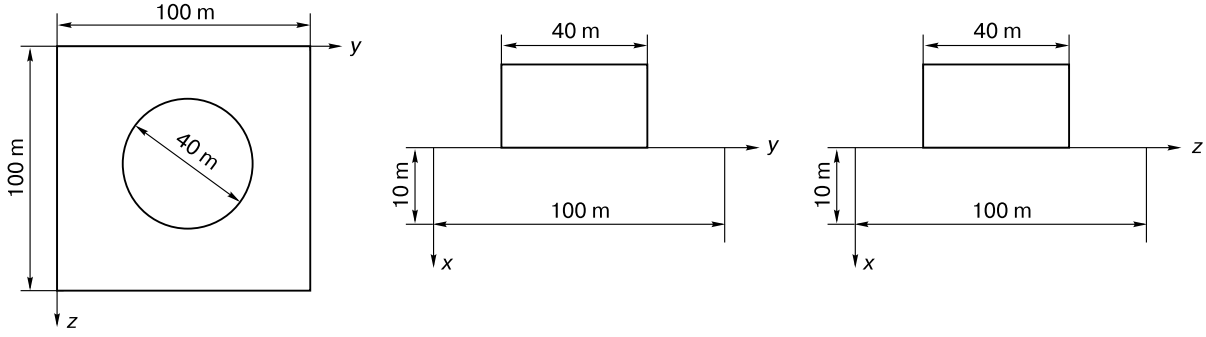

Fig. 1. Block diagram of the computational domain and oil tank area.

PROBLEM FORMULATION

The effective heat capacity method was used to calculate heat and mass transfer in soils, where heat-transfer equation is presented in the following form [*Samarskii and Vabishchevich, 2003*]:

$$\left[C + L\delta\left(t - t_{\text{p}}\right)\right]\frac{\partial t}{\partial \tau} = \lambda\left(\frac{\partial^2 t}{\partial x^2} + \frac{\partial^2 t}{\partial y^2} + \frac{\partial^2 t}{\partial z^2}\right), \qquad (1)$$

where C is volumetric heat capacity of soil; λ is coefficient of heat conductivity of soil; t – temperature;

t_p – phase transition temperature; x, y, z are Cartesian coordinates (orthogonal coordinates); τ is time; $\delta(t - t_p)$ is Dirac delta function. The values of L are derived from the expression:

$$L = r(w - w_{uw})\gamma_{ss},$$

where r is specific heat of fusion of ice; w is soil moisture; w_{uw} is moisture content in unfrozen water; γ_{ss} is apparent density of soil skeleton.

The difference scheme, corresponding to the equation (1) is written down as follows:

$$t(i,j,k,n+1) = t(i,j,k,n) +$$

$$+\frac{a(i,j,k)h_\tau}{h_x^2}\left[t(i+1,j,k,n)+t(i-1,j,k,n)-2t(i,j,k,n)\right]+$$

$$+\frac{a(i,j,k)h_\tau}{h_y^2}\left[t(i,j+1,k,n)+t(i,j-1,k,n)-2t(i,j,k,n)\right]+$$

$$+\frac{a(i,j,k)h_\tau}{h_z^2}\left[t(i,j,k+1,n)+t(i,j,k-1,n)-2t(i,j,k,n)\right],$$

where

$$a(i,j,k) =$$

$$= \begin{cases} a_f, & t(i,j,k,n) < t_p - \Delta, \\ \dfrac{0.5(\lambda_f + \lambda_t)}{0.5(c_f + c_t) + L/2\Delta}, & t_p - \Delta \le t(i,j,k,n) \le t_p + \Delta, \\ a_t, & t(i,j,k,n) > t_p + \Delta. \end{cases}$$

Here, a_t, a_f is thermal diffusivity of thawed and frozen ground, respectively; λ_t, λ_f is thermal conductivity coefficient of thawed and frozen ground; c_t, c_f are specific heat capacities of thawed and frozen ground; t_p is phase transition temperature.

In the effective heat capacity method, the value of Δ [*Samarskii and Vabishchevich, 2003*] defines the range of temperatures, over which the phase transition occurs: $t_p - \Delta \le t(i, j, k, n) \le t_p + \Delta$. When calculating $a(i, j, k)$ the Dirac delta function in the expression (1) is replaced by the function $f(t - t_p)$, and is given by the following expressions [*Samarskii and Vabishchevich, 2003*]:

$$f(t - t_p) = \begin{cases} 0, & |t - t_p| > \Delta, \\ \dfrac{1}{2\Delta}, & |t - t_p| \le \Delta. \end{cases}$$

The grid of spatial and temporal coordinates in the computational domain and stability criterion for the explicit difference scheme, are given as

$$x_i = ih_x,\ 0 \le i \le i_{max},$$

$$y_i = jh_y,\ 0 \le j \le j_{max},$$

$$z_k = kh_z,\ 0 \le k \le k_{max},$$

$$\tau_n = h_\tau n,\ 0 \le n \le n_{max},$$

$$h_\tau \le \frac{1}{3a}\left(\frac{1}{h_x^2} + \frac{1}{h_y^2} + \frac{1}{h_z^2}\right)^{-1}.$$

Here, $a = \max(a_t, a_f)$; h_x, h_y, h_z are step size values for x, y, z-coordinates, respectively; h_τ is time increment (the time step); i_{max}, j_{max}, k_{max} are maximum values of i, j, k, setting the size of computational domain; n_{max} defines the point of time, at which the temperature field is determined.

The soil surface – atmosphere thermal interaction depends mostly on the thermal effects of radiation and convective heat transfer. The heat flow controlling the influence of radiation on the surface of soil or snow, is given by the following expression [*Pavlov, 1984*]

$$q_r = R(1 - A) - \varepsilon\sigma T_s^4(1 - p),$$

where q_r is radiative heat flux; R is direct solar radiation; A is albedo; σ is Stefan–Boltzmann constant; T_s is temperature of the Earth's surface; p is the proportion of infrared radiation (thermal infrared energy) emitted by the surface and reflected by the atmosphere back to the earth's surface; ε is coefficient representing the level of the surface dullness.

According to [*Pavlov, 1984*], the coefficient of dullness may be accepted close to 1, and p variables average at 0.84 throughout the globe [*Trenberth et al., 2009*]. This value in our case is unknown, but given that its contribution to the overall heat flow rate appears not a governing parameter, its average at the Earth's surface can be used for the calculations.

The flux of convective heat from the atmosphere to the ground or snow surface is given by the following expression [*Foken, 2008*]:

$$q_c = \frac{\rho c_p(\alpha_0\kappa)^2 v(z)(t(z) - t(0))}{(\ln(z/z_0))^2}. \qquad (2)$$

Here, q_c is convection-driven heat flux; ρ is air density; c_p is specific heat capacity of the air; $\alpha_0 = 1.25$; $\kappa = 0.4$ represents karman constant; $v(z)$ is air velocity at height z from the surface; $t(z)$ is temperature at height z; $t(0)$ is surface temperature.

Normally, the temperature measurements are taken at a height of about 2 m and the wind speed at 10 m. In order to obtain the resultant expression, it should be taken into account that the following relation is satisfied [*Foken, 2008*]

$$v(z) = v(10)\frac{\ln(z/z_0)}{\ln(10/z_0)}. \qquad (3)$$

Substituting (3) into (2), we obtain the resultant expression for the convective heat flux

$$q_c = \frac{\rho c_p(\alpha_0\kappa)^2 v(10)(t(z) - t(0))}{\ln(z/z_0)\ln(10/z_0)},$$

where z is the height at which the atmospheric temperature is measured at the meteorological station;

z_0 is the parameter allowing for the surface roughness. The greater is the surface roughness, the bigger is z_0. For a smooth surface cover, such as snow, we have $z_0 = 0.001$ m, and $A = 0.75$, whereas for soil $z_0 = 0.02$ m, $A = 0.25$ [*Pavlov, 1984*].

The values of normal beam solar radiation were taken from [*Pavlov, 1984*]:

Month	I	II	III	IV	V	VI	VII	VIII	IX	X	XI	XII
R, W/m^2	0	16	74	171	205	237	224	129	60	22	3	0

Thermal boundary conditions at the surface of soil are written as

$$q_r + q_c = -\lambda \frac{\partial t}{\partial x},$$

where λ is the thermal conductivity of the material verging on the air (either snow, or ground); x is depth.

Fig. 2 represents a schematic diagram of boundary conditions in the computational domain.

The boundary condition used for the side surfaces of the computational domain is $q_n = 0$ (q_n is heat flow normal to the side surface of the computational domain). The boundary condition of the first kind is set at the lower boundary of the computational domain.

A coordinate grid is normally selected so that the nodes of lattices pass through the pipes of the cooling system (they are considered to be a linear source of cold). The thermal flow entering the node through which passes the evaporator tube of the system is quite easy to calculate, as it is numbered with i, j, k at the x, y, z-coordinates, respectively, and is given by

$$U_{i,j,k} = \frac{\lambda_{\text{gr}} h_x h_z}{h_y}\left(t_{i,j+1,k} + t_{i,j-1,k} - 2t_{\text{e}}\right) + \frac{\lambda_{\text{gr}} h_y h_z}{h_x}\left(t_{i+1,j,k} + t_{i-1,j,k} - 2t_{\text{e}}\right),$$

where λ_{gr} is thermal conductivity of the soil; t_{e} is temperature of the evaporator tube.

The heat exchange between the evaporator of the soil temperature stabilization system (STS) and the atmosphere is set with the given boundary condition

$$\sum_{i,j,k \in M} U_{i,j,k} = S_{\text{con}} N_{\text{con}} \eta_{\text{ef}} \left(t_{\text{c}} - t_{\text{a}}\right)\alpha,$$

where M is the set of nodes of computational grid the computer system tubes pass through; S_{con} is the area of condenser unit; N_{con} is the number of condenser units; η_{ef} is fin efficiency; t_{c} is the temperature of the condenser; t_{a} is the atmospheric temperature; α is heat-exchange coefficient of the condenser.

As follows from [*Anikin and Spasennikova, 2012*], the condenser temperature can be determined, given the temperature of evaporator is known, which, in turn, is equal to the soil temperature at the soil – evaporator pipe interface:

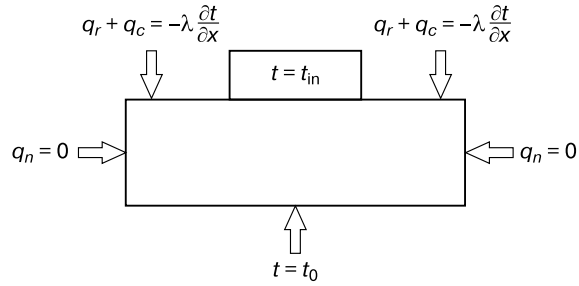

Fig. 2. Schematics of boundary conditions in the computational domain (t_{in} – indoor temperature).

$$t_{\text{c}} = t_{\text{e}} - \frac{0.5\rho_{\text{ca}} g H}{dP_{\text{sat}}/dt},$$

where t_{e} – temperature of the evaporator tube; ρ_{ca} – the density of refrigerant; g – acceleration of gravity; H is height of the condenser above evaporator; dP_{sat}/dt is the derivative of saturation pressure with respect to temperature.

When compared earlier, the discribed methodology for calculations and the thermometric data showed good agreement [*Dolgich et al., 2013*]. In the heat transfer simulations, the probabilistic nature of meteorological parameters will be taken into account. Average capacity per condensing unit during the winter period is given by the following expression:

$$\bar{U} = \frac{Q}{n n_{\text{c}} \cdot 3600 \cdot 24}.$$

Here, $\bar{U}$ is average capacity per a condensing unit during the winter period; Q is cumulative heat transferred from soil to the atmosphere by "GET" systems; n is the number of days when the temperature was negative during the year; n_{c} – number of condensing units. Average capacity during the winter period should be distinguished from average working capacity, which is given by the following expression:

$$\langle U \rangle = \frac{Q}{m n_{\text{c}} \cdot 3600 \cdot 24}.$$

Here, $\langle U \rangle$ is average operating capacity per one condensing unit; m – number of days per year when the "GET" systems were running, i.e. the number of days in which the temperature of evaporator tubes was higher than the atmospheric temperature.

In this example, as follows from [*Anikin and Spasennikova, 2012*], the ground cooling system with ten (10) standard condensers of NPO "Fundamentstroyarkos", OOO manufacture was used, therefore, $n_{\text{c}} = 10$.

ANALYSIS OF THE IGARKA WEATHER STATION DATA

According to the meteorological data measured at Igarka weather station the probability distribu-

tions of temperature and wind speed were obtained. It proved to be the case that the probability distribution of temperatures is described well by a normal distribution

$$w(t) = \frac{\exp\left(-\left(t-\overline{t}\right)^2 / 2\sigma_t^2\right)dt}{\sqrt{2\pi}\sigma}, \qquad (4)$$

where t is temperature; $\overline{t}$ is mathematical expectation; σ_t is root-mean-square deviation. The wind speed probability (stochastic) distribution is described by a gamma-distribution:

$$w(v) = \frac{\lambda^\alpha}{\Gamma(\alpha)} v^{\alpha-1} e^{-\lambda v} dv, \qquad (5)$$

where v is the wind speed; $\Gamma(\alpha)$ is gamma function; α and λ are aligned to the mean wind speed and Dv variance by the following relations:

$$\overline{v} = \alpha/\lambda, \quad Dv = \alpha/\lambda^2.$$

Comparisons of the distributions obtained from the Igarka weather station archive data with similar distributions obtained using random number generators program *MathCAD-14* for March and September are shown in Fig. 3.

A similar agreement between the Igarka weather station archive data and the data obtained using random number generators, was markedly observable in wind speed and air temperature values for other months (Table 1).

Due to a small sample size of the archived data, we were unable to obtain a smooth distribution of the snow cover thickness, which is why it was modeled using normal mathematical expectation $\overline{h}$ and root-mean squared deviation σ_h, given by the following formulas:

$$\overline{h} = \sum_i \frac{h_i}{N}, \quad \sigma_h = \sqrt{\sum_i \frac{\left(h_i - \overline{h}\right)^2}{N}}.$$

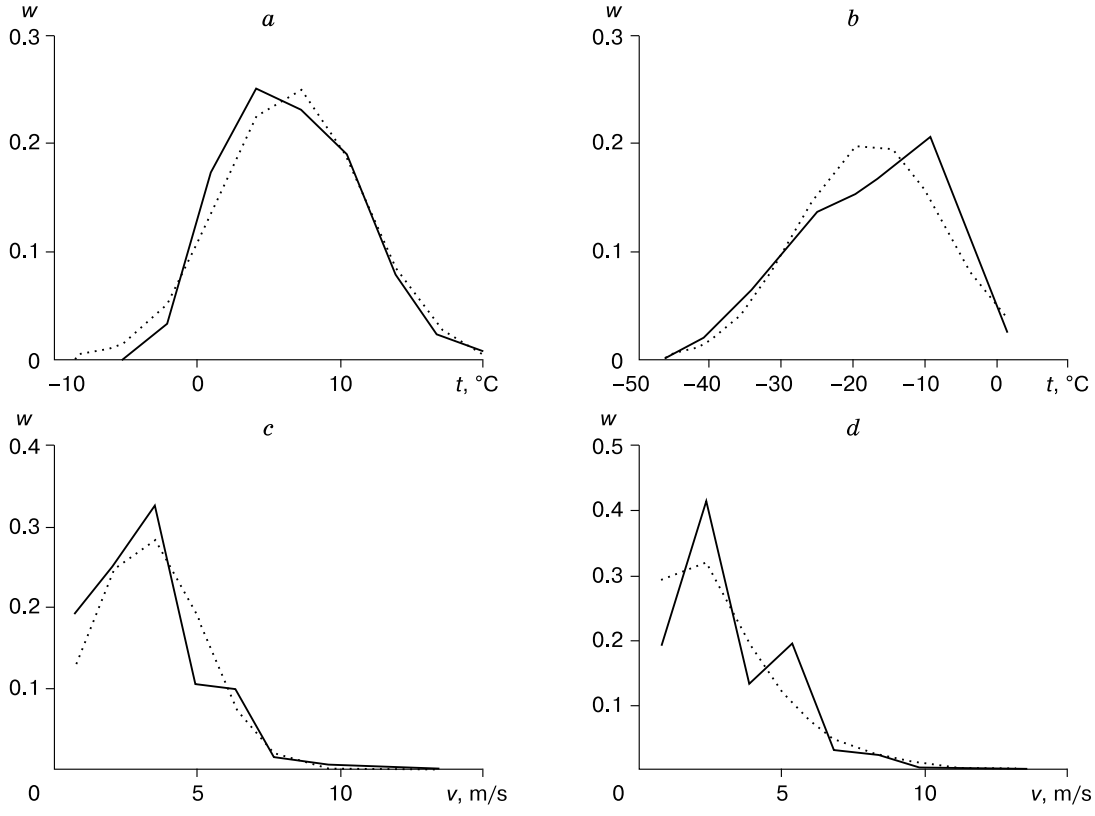

Fig. 3. Temperatures versus wind speed distributions for September and March, according to the archive data from Igarka Weather Station for the period of 2007–2012, with similar distributions obtained using *MathCAD-14* program random number generators.

a: solid line is for the temperature distributions in September; dotted line is for normal distribution with σ = 4.86 °C, $\overline{t} = -4.2$ °C, obtained with a random number generator; *b*: solid line is for the temperature distributions in March; dotted line is for normal distribution with σ = 10.2 °C, $\overline{t} = -17.3$ °C, obtained with a random number generator; *c*: solid line is for wind speed distributions in September, dotted line is for gamma distributions with α = 2.77, λ = 0.88, obtained from a random number generator; *d*: solid line is for wind speed distributions in March, the dotted line is for gamma distributions; solid line – the distribution of wind speed in March, the dotted – gamma distribution α = 1.91, λ = 0.64, obtained from a random number generator.

Table 1. **Distribution parameters for each month**

Parameter	Jan.	Feb.	March	Apr.	May	June	July	Aug.	Sept.	Oct.	Nov.	Dec.
$\bar{t}$, °C	–26.20	–27.00	–17.30	–8.12	–0.66	11.20	15.80	11.30	6.60	–4.20	–19.10	–24.40
σ_t, °C	10.80	9.88	10.20	9.24	6.34	5.99	5.18	4.41	4.86	7.29	11.13	11.40
α	1.61	1.54	1.91	2.40	3.66	4.54	2.15	2.68	2.77	2.84	1.58	2.18
λ, s/m	0.59	0.60	0.64	0.75	1.06	1.39	0.91	0.94	0.88	0.87	0.59	0.70
$\bar{h}$, m	0.70	0.79	0.86	0.79	0.48	0	0	0	0	0.12	0.35	0.53
σ_h, m	0.21	0.19	0.19	0.20	0.22	0	0	0	0	0.10	0.13	0.17

Here, the summation is performed for the entire sample size; h_i is particular value of the snow cover thickness in the sample for the given month; N is sample size for a given month $\bar{h}$ and σ_h values for each month are provided in Table 1. For the summer months including September, when there was no snow cover, they were accepted as $\bar{h} = 0$, $\sigma_h = 0$.

EXPERIMENTAL DETERMINATION OF HEAT TRANSFER COEFFICIENT OF FINNED SURFACE OF THE CONDENSER

The output transferred from the condensing unit to the atmosphere is given by

$$U = S\eta_{ef}\alpha_c(t_c - t_a), \quad (6)$$

where S is the area of finned section; η_{ef} – effectiveness ratio of fins; α_c – heat transfer coefficient of the condenser unit; t_c is temperature of the condenser; t_a is the atmospheric temperature. For standard unit S = 110 m^2; η_{ef} = 0.95. The value of α_c was determined from the analysis of experimental data on the testing area of NPO "Fundamentstroyarkos", OOO, and the results are provided in Table 2.

The experiment rationale consisted in the predetermined heat load q_i delivered to the insulated tube of the evaporator system with length L = 272 m by means of electric heating, with simultaneously measured temperature of the condenser unit t_{ci}, atmospheric temperature t_{ai} and wind speed v_i. At that, the value of heat transfer coefficient of the condenser α_c was determined for each measurement marked with i-number, using the formula (6) and the relation $U = qL$, using the expression

$$\alpha_{ci} = \frac{q_i L}{S\eta_{ef}(t_{ci} - t_{ai})}.$$

When applying statistical analysis to the relation of random variables α_{ci} and v_i [*Efimova et al., 1998*], we obtain the linear regression equation that specifies the relationships between α_c and v:

$$\alpha_c = 2.42 + 2.1v. \quad (7)$$

Moreover, the coefficient of correlation between these two values is equal to 0.82 [*Efimova et al., 1998*]. This suggests that the equation (7) proves statistically significant and thus can be readily used. Knowing the heat transfer coefficient, derived from the equation (7), and the dependence of the condenser/evaporator temperatures [*Anikin et al., 2011*], we can calculate the atmosphere – soil heat exchange process.

Table 2. **Experimental data obtained at the NPO "Fundamentstroyarkos", OOO testing ground**

i	q_i, W/m	t_{ci}, °C	t_{ai}, °C	v_i, m/s
1	5	1.2	–1.0	1.0
2	5	–0.8	–1.6	2.5
3	5	4.2	–4.8	0.5
4	5	2.8	–8.6	0.2
5	10	3.5	–3.0	1.0
6	10	–0.6	–4.5	1.5
7	10	–2.0	–6.6	4.0
8	10	–1.4	–5.7	0.1
9	15	–5.5	–15.8	1.5
10	14.78	–9.7	–15.1	4.0
11	20.38	–8.3	–10.4	10.0
12	20.91	–7.9	–10.0	6.5
13	20.51	–7.8	–10.4	9.0
14	21.18	–0.6	–7.5	5.3
15	21.31	–0.8	–6.1	6.2
16	21.44	–2.6	–8.0	3.0

Note. i is the number of measurement; q_i is specific heat load; t_{ci} is temperature of the condenser unit; t_{ai} is atmospheric temperature; v_i – wind speed.

STOCHASTIC FORECASTS FOR SOIL TEMPERATURES AND OUTPUT RATES OF "GET" SYSTEMS

Using the distributions (4) and (5) conjugated with the parameters from Table 1, the 48 future processes scenarios were calculated, using Monte-Carlo method. The calculation was performed for two-year period spanning from the beginning of September in the first year till the end of August in the second year. Thus, the 48 calculated values of $\bar{U}$, $\langle U \rangle$, n, m have been obtained and are provided in Table 3.

Table 3. **Future processes scenarios for variables $\bar{U}, \langle U \rangle, n, m$**

Scenario i	$\bar{U}_i$, kW	$\langle U \rangle_i$, kW	n_i, day	m_i, day
0	2.010	3.032	227.5	150.7
1	2.456	3.465	212.0	150.3
2	2.413	4.006	227.5	137.0
3	1.956	3.137	243.0	151.5
4	2.485	4.995	227.5	113.2
5	2.494	3.362	196.5	145.8
6	2.498	3.576	196.5	137.2
7	2.028	3.779	211.5	113.5
8	2.098	3.675	258.0	147.3
9	1.943	3.135	212.0	131.4
10	2.407	4.262	227.5	128.5
11	1.780	2.974	242.5	145.2
12	2.347	3.906	227.5	136.7
13	2.495	3.677	197.5	134.0
14	2.384	3.745	227.5	144.8
15	2.202	3.136	227.0	159.4
16	2.178	2.865	197.0	149.8
17	2.156	3.144	212.0	145.4
18	2.196	5.126	227.0	97.3
19	2.414	3.184	212.5	161.1
20	2.233	4.308	212.0	109.9
21	2.248	3.977	212.0	119.8
22	1.557	3.027	242.5	124.8
23	2.470	3.493	212.0	149.9
24	2.705	4.408	181.0	111.1
25	1.794	3.472	242.5	125.3
26	1.892	2.961	227.5	145.3
27	2.053	3.796	212.0	114.7
28	2.261	4.218	242.5	130.0
29	2.414	3.654	212.0	140.1
30	2.461	3.940	243.0	151.8
31	2.657	4.126	212.0	136.5
32	2.342	3.369	212.0	147.4
33	2.558	3.293	212.0	164.7
34	1.601	2.358	242.5	164.6
35	2.320	4.164	227.5	126.8
36	2.293	3.269	212.0	148.7
37	2.662	5.335	242.5	121.0
38	2.097	3.831	242.5	132.8
39	2.384	4.311	227.5	125.8
40	2.483	3.885	212.0	135.5
41	2.379	3.247	227.5	166.7
42	2.240	3.440	227.5	148.2
43	2.222	3.482	227.5	145.2
44	2.574	4.550	212.0	120.0
45	1.858	2.783	227.5	151.9
46	1.830	2.631	242.5	168.7
47	2.489	6.014	212.0	87.7

For each of the above variables their average values have been found:

$$\bar{U}_{\text{av}} = \frac{1}{48}\sum_{i=0}^{47}\bar{U}_i = 2.25\ \text{kW},\ \langle U \rangle_{\text{av}} = \frac{1}{48}\sum_{i=0}^{47}\langle U \rangle_i = 3.698\ \text{kW},$$

$$n_{\text{av}} = \frac{1}{48}\sum_{i=0}^{47} n_i = 222.25\ \text{day},\ m_{\text{av}} = \frac{1}{48}\sum_{i=0}^{47} m_i = 137.38\ \text{day}$$

as well as root-mean-square deviation of these values

$$\sigma_{\bar{U}} = \sqrt{\frac{1}{48}\sum_{i=0}^{47}\left(\bar{U}_i - \bar{U}_{\text{av}}\right)^2} = 273.5\ \text{W},$$

$$\sigma_{\langle U \rangle} = \sqrt{\frac{1}{48}\sum_{i=0}^{47}\left(\langle U \rangle_i - \langle U \rangle_{\text{av}}\right)^2} = 708.2\ \text{W},$$

$$\sigma_n = \sqrt{\frac{1}{48}\sum_{i=0}^{47}\left(n_i - n_{\text{av}}\right)^2} = 15.74\ \text{day},$$

$$\sigma_m = \sqrt{\frac{1}{48}\sum_{i=0}^{47}\left(m_i - m_{\text{av}}\right)^2} = 17.85\ \text{day}.$$

Table 4. **Probability of finding specific variable value within the given interval**

Limit of range		Probability
lower	upper	
Variable $\bar{U}$, kW		
1.557 30	1.786 88	0.0625
1.786 88	2.016 46	0.145 833 333
2.016 46	2.246 04	0.229 166 667
2.246 04	2.475 62	0.333 333 333
2.475 62	2.705 20	0.229 166 667
Variable $\langle U \rangle$, kW		
2.357 91	3.089 20	0.166 666 670
3.089 20	3.820 48	0.458 333 333
3.820 48	4.551 77	0.291 666 667
4.551 77	5.283 05	0.041 666 667
5.283 05	6.014 34	0.041 666 667
Variable n, day		
181.0	196.4	0.020 833 333
196.4	211.8	0.104 166 667
211.8	227.2	0.375
227.2	242.6	0.4375
242.6	258.0	0.0625
Variable m, day		
87.735	103.924	0.041 666 667
103.924	120.113	0.145 833 333
120.113	136.302	0.229 166 667
136.302	152.491	0.458 333 333
152.491	168.680	0.125

Therefore, the 65 % probability for normal probability distribution can be written as

$$\bar{U} = (2.250 \pm 0.274)\,\text{kW}, \quad \langle U \rangle = (3.698 \pm 0.701)\,\text{kW},$$

$$n = (222.25 \pm 15.74)\,\text{day}, \quad m = (137.38 \pm 17.85)\,\text{day}.$$

We now calculate the probability of finding each of these variables. The data processing using *MathCAD* software yielded the following results (Table 4):

– the relation satisfied with probability 79 % is:

$$2.02\,\text{kW} \le \bar{U} \le 2.71\,\text{kW};$$

– the relation satisfied with probability 75 % is:

$$3.09\,\text{kW} \le \langle U \rangle \le 4.55\,\text{kW};$$

– the relation satisfied with probability 81 % is:

$$211.8\,\text{day} \le n \le 242.6\,\text{day};$$

– the relation satisfied with probability 67 % is:

$$120.1\,\text{day} \le m \le 152.5\,\text{day}.$$

Considering temperature distributions with depth in the area beneath the center of the oil tank, the coldest and warmest options are given in Fig. 4. Temperature fields at a depth of buried pipes in scenarios 22 and 37 are shown in Fig. 5, *a*, *b*, respectively.

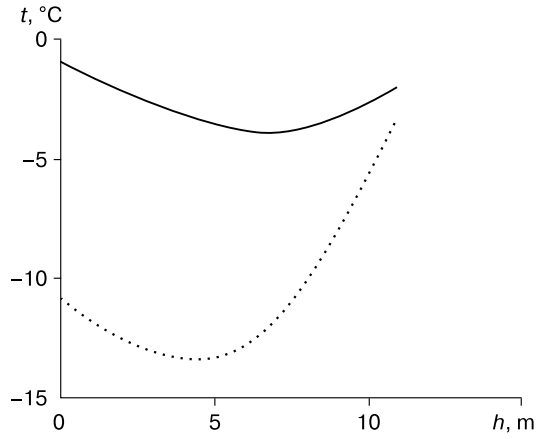

Fig. 4. Distribution of temperature (*t*, °C) with depth (*h*, m) for the coldest and warmest scenarios in late August.

Solid line is for temperature distribution with depth for scenario 22 from Table 2 (the warmest), dotted line is for the temperature distribution with depth in scenario 37 from Table 2 (the coldest).

CONCLUSION

The performed calculations have shown that the results spread for different scenarios is quite substantial. This fact casts doubt on the possibility of providing an adequate forecast of the ground conditions for such systems as "GET" by utilizing every year the same variables, as average monthly air temperature, wind speed and snow depth. The stochastic forecast introduced in this paper allows to define the worst (the warmest) option and to develop the worst case scenario-based foundation design. It should also be noted that the calculations were performed on a supercomputer NCC-30T + GPU at Siberian Supercomputer Center.

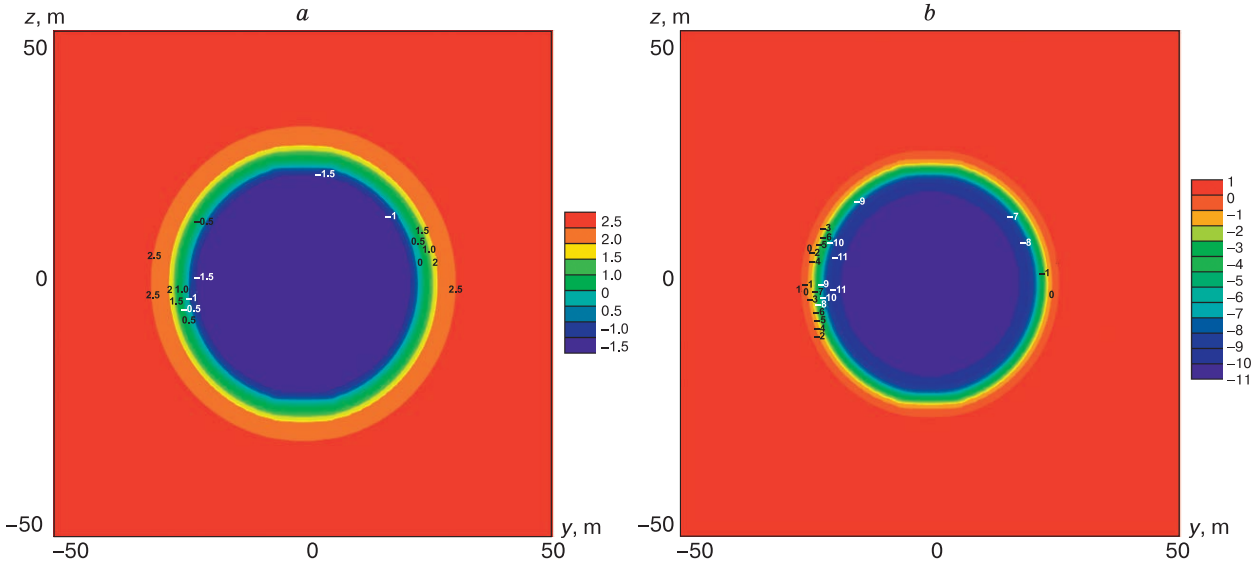

Fig. 5. End of August temperature distributions at the depth of buried pipes.

a – scenario 22 (the warmest in the center); *b* – scenario 37 (the coldest in the center). The pipes of the cooling system run parallel to axis *z*.

References

Anikin, G.V., Plotnikov, S.N., Spasennikova, K.A., 2011. Computer simulations of heat and mass transfer in horizontal systems of soil temperature cooling. Kriosfera Zemli XV (1), 33–39.

Anikin, G.V., Spasennikova, K.A., 2012. Computer simulations of ground cooling system under oil tanks. Kriosfera Zemli XVI (2), 60–64.

Dolgich, G.M., Okunev, S.N., Podenko, L.S., Felikstov, V.N., 2008. Reliability, efficiency and manageability of thermostabilization systems for ground foundations of buildings and facilities in the permafrost areas, in: Proceedings of International Conference "Cryogenic Resources of Polar and Mountainous Regions. Current State and Outlook for Permafrost engineering", Tyumen, pp. 34–39. (in Russian)

Dolgich, G.M., Okunev, S.N., Anikin, G.V., Spasennikova, K.A., 2013. Computations of non-steady temperature fields in the oil tank-seasonal ground cooling plant system. Kriosfera Zemli XVII (3), 70–75.

Efimofa, M.R., Petrova, E.V., Rumyantsev, V.N., 1998. General theory of statistics. INFRA-M, Moscow, 413 pp. (in Russian)

Foken, T., 2008. Micrometeorology. Springer, Berlin, 306 pp.

Pavlov, A.V., 1984. Energy Exchange in Earth's Landscape Sphere. Nauka, Novosibirsk, 256 pp. (in Russian)

Samarskii, A.A., Vabishchevich, P.N., 2003. Heat-transfer Computing. Editorial, URSS, Moscow, 784 pp. (in Russian)

Trenberth, K.E., Fasullo, J.T., Kienl, J., 2009. Earth's global energy budget. Amer. Meteorol. Soc., No. 3, pp. 311–323.

Received June 27, 2013